

High-Current Low-Pressure Quasi-Stationary Discharge in a Magnetic Field: Experimental Research

D. V. Mozgrin, I. K. Fetisov, and G. V. Khodachenko

Moscow Engineering Physics Institute, Kashirskoe sh. 31, Moscow, 115409 Russia

Received October 22, 1993; in final form, July 12, 1994

Abstract – The possibility of realizing several types of high-power quasi-stationary low-pressure discharge in a magnetic field was shown. Two noncontracted discharge regimes in crossed \mathbf{E} and \mathbf{H} fields were studied. These discharges had much higher cathode current densities than those of other known discharge types. Their parameter ranges were determined, and their operating regimes were investigated. The voltage for the high-voltage form discharge ranged from 450 to 1000 V; the discharge current amounted to 250 A, and cathode current density reached 25 A/cm². A low-voltage discharge form was first observed: voltage ranged from 75 to 120 V; discharge current amounted to 1800 A, and cathode current density reached 75 A/cm²; lifetime was about 1.5 ms. The ion density was 1.5×10^{15} cm⁻³ in argon discharges and amounted to 5×10^{14} cm⁻³ in He-H₂-mixture discharges, while the electron temperature was about 3 - 8 eV. The properties of both discharge types are expected to open up new fields of application in technology.

1. INTRODUCTION

Low-pressure discharges in a magnetic field attract much attention due to their wide use in technological magnetron devices, closed-electron-drift plasma accelerators, and, as plasma emitters in electron or ion injectors.

Stationary regimes of the discharges in planar magnetrons of technological use are characterized by $p = 10^{-4} - 5 \times 10^{-2}$ torr operating pressure and 300 - 1000 G magnetic field at the cathode surface [1, 2]. Their AV characteristic is described by the formula $I_d = kU_d^n$, where I_d is the discharge current, and U_d is the discharge voltage. The quantities k and n depend on the device geometry, working gas type and pressure, and magnetic field strength. The condition $n > 1$ holds, if the cathode current density j_c does not exceed 0.03 A/cm². In this case the discharge voltage amounts to 400 - 600 V, the plasma density n_i ranges from 10^8 to 10^{11} cm⁻³, and electron temperature T_e reaches 20 eV. If the current density is higher, a transition of the discharge into the arc regime is observed.

Because of the need for greater discharge power and plasma density, pulse or quasi-stationary regimes appear to be of interest. Some experiments on magnetron systems of various geometry showed that discharge regimes which do not transit to arcs can be obtained even at high currents. For example, a superdense glow discharge, realized in a device of "reversed-magnetron" type of coaxial geometry, exhibited the following parameters: about 70 A discharge current I_d , 400 V discharge voltage U_d , 60 μ s pulse duration, and 10^{12} cm⁻³ plasma density n_i [3]. A pulse duration decrease down to 100 μ s, which was performed in a planar magnetron discharge in Ar, N₂, or H₂ at $10^{-3} - 5 \times 10^{-2}$ torr

pressures and 1.0 - 3.0 kG magnetic field strength, permitted a 1000 A current value to be obtained in the noncontracted regime, at 300 - 500 V discharge voltage, with about 50 J of total energy deposition [4]. In both examples, the discharge current-voltage characteristic increased and then became constant with the increase in the discharge currents. A further increase in the discharge currents caused the discharges to transit to the arc regimes, with voltage not higher than 50 V under those conditions.

Our previous experiments demonstrated the possibility of realizing several stable discharge regimes in devices with closed electron drift [5 - 7]. Among these regimes which differed from the arcs, was an intermediate low-voltage regime ($U_d \approx 100$ V, $I_d \leq 1.5$ kA) of longer than 1-ms pulse duration (hereafter called a "high-current diffuse regime").

The main purpose of this work was to study experimentally a high-power noncontracted quasi-stationary discharge in crossed fields of various geometry and to determine their parameter ranges. We investigated the discharge regimes in various gas mixtures at $10^{-3} - 10$ torr, $B_0 \leq 1000$ G, and pulse durations exceeding 1 ms. Such regimes can be useful in generating large-volume dense plasmas and intense flows of charged particles. Furthermore, we consider qualitatively the mechanism of low-voltage high-current discharge formation.

2. EXPERIMENT

To study the high-current forms of the discharge, we used two types of devices: a planar magnetron and a system with specifically shaped hollow electrodes.

The planar magnetron (Fig. 1) involved a plane cathode 120 mm in diameter and a ring-shaped anode

160 mm in diameter. The electrodes were immersed in a magnetic field of annular permanent magnets. Magnetic circuits were used to vary the size of the region of the large magnetic-field radial component and magnetic field inhomogeneity degree. To control the magnetic field strength at the cathode surface, we displaced the magnetic system along the axis z (Fig. 1) and used two types of permanent magnets made of SmCo_5 and NdFeB . The discharge had an annular shape and was adjacent to the cathode. The maximum of the magnetic field radial component B_r at the cathode surface was 800 G for the SmCo_5 magnet or 1200 G for the NdFeB magnet. The cathodes we used were made of Cu, Mo, Ti, Al, or stainless steel. The cathode was placed on a cooled surface. The anodes were made of aluminum or stainless steel.

The system with shaped electrodes involved two hollow axisymmetrical electrodes 120 mm in diameter, separated by about 10 mm, and immersed in a cusp-shaped magnetic field produced by oppositely directed multilayer coils. The discharge volume bounded by the electrodes was about 10^3 cm^3 . The ratio of the maximal magnetic field at the axis of symmetry $B_{\text{max}}(z, 0)$ to the maximal magnetic field at the plane of symmetry $B_{\text{max}}(0, r)$ was about 3. The values of B_{max} were controlled by coil current variation to range from 0 to 1000 G. The electrode shapes followed the magnetic line profile, which enabled the electric field to be perpendicular to the magnetic field along the cathode surface. Such a field configuration allowed us to combine a high-current magnetron discharge with a hollow-cathode discharge.

The gas from the discharge volume was pumped out; minimal residual gas pressure was about 8×10^{-6} torr.

It was possible to form the high-current quasi-stationary regime by applying a square voltage pulse to the discharge gap which was filled up with either neutral or pre-ionized gas. Estimates were made to determine both the quasi-stationary plasma density and its building-up time [5, 7]. The necessary pre-ionized plasma density n_i turned out to be $10^7 - 10^9 \text{ cm}^{-3}$ for argon. In addition, the estimates determined the shape and parameters of the voltage pulse. The pre-ionization could be provided by RF discharge, anomalous glow or magnetron discharge, etc.

Figure 2 presents a simplified scheme of the discharge supply system. The supply unit involved a pulsed discharge supply unit and a system for pre-ionization. The quasi-stationary discharge-supply unit consisted of a long line of $W = 5.5 \text{ kJ}$ maximal energy content, a switch, and a matching unit. The pre-ionization system provided direct current up to 0.3 A and voltage up to 3 kV.

The frequency parameters of the pulsed supply unit were chosen in accordance with the increase in time of the quasi-stationary plasma density formation and the times of the ionization instability and ionization-overheating instability development. Designing the unit, we

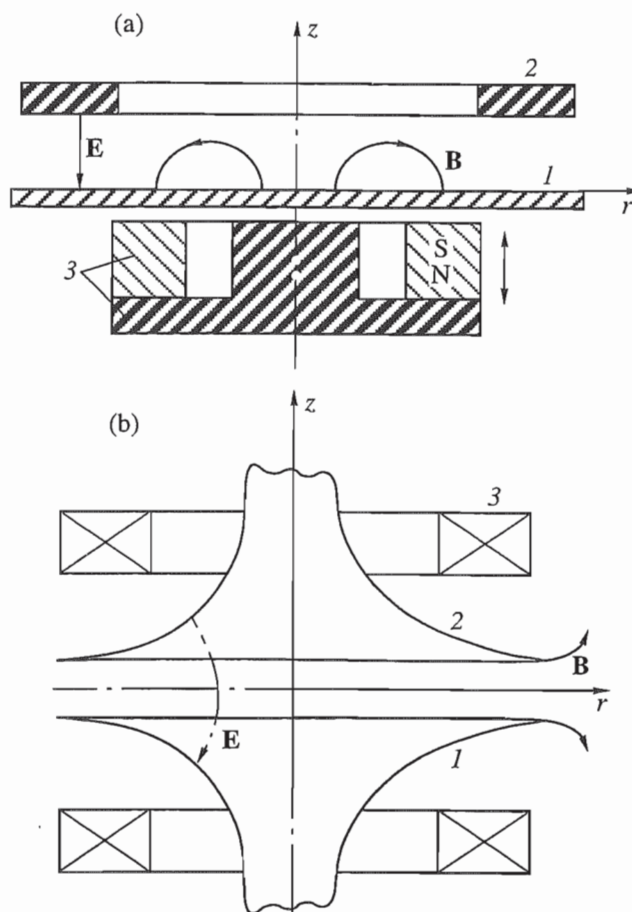


Fig. 1. Discharge device configurations: (a) planar magnetron; (b) shaped-electrode configuration. (1) Cathode; (2) anode; (3) magnetic system.

took into account the dependences which had been obtained in [8] of ionization relaxation on pre-ionization parameters, pressure, and pulse voltage amplitude. In addition, we allowed for the fact that the development time for the ionization-overheating instability was about $10^{-3} - 3 \times 10^{-3} \text{ s}$ in the pressure range up to 0.5 torr [9]. Thus, the supply unit was made providing square voltage and current pulses with raise times (leading edge) of 5 - 60 μs and durations of as much as 1.5 ms. Short-circuit current amplitude was up to 3 kA; no-load voltage was as much as 2.4 kV.

For pre-ionization, we used a stationary magnetron discharge; the discharge current ranged up to 300 mA. We measured the discharge current-voltage characteristics (CVC) in a $10^{-3} - 10$ torr pressure range and plasma parameters of the discharge at the symmetry center of the shaped-electrode system using a probe technique. We found out that only the regimes with magnetic field strength not lower than 400 G provided the initial plasma density in the $10^9 - 10^{11} \text{ cm}^{-3}$ range. This initial density was sufficient for plasma density to grow when the square voltage pulse was applied to the gap. So we chose these regimes as pre-ionization regimes.

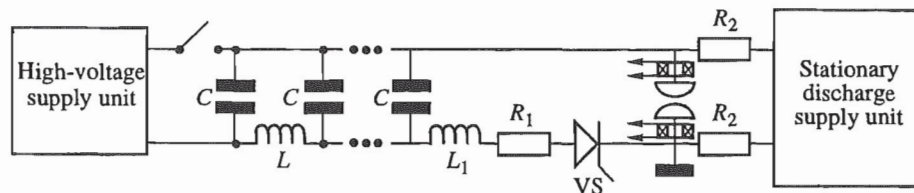


Fig. 2. Discharge supply unit.

3. QUASI-STATIONARY DISCHARGE REGIMES

We studied the high-current discharge in wide ranges of discharge current (from 5 A to 1.8 kA) and operating pressure (from 10^{-3} to 10 torr) using various

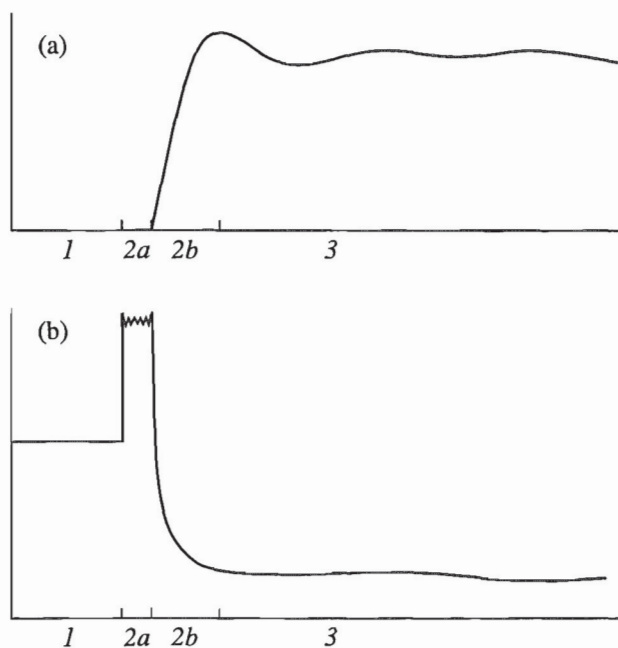


Fig. 3. Oscillograms of (a) current and (b) voltage of the quasi-stationary discharge (50 μ s per div., 180 A per div., 180 V per div.).

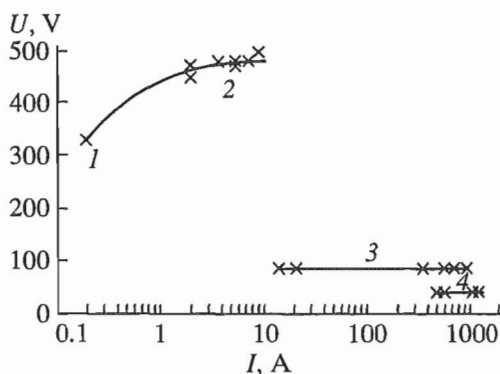


Fig. 4. Current-voltage characteristic of the quasi-stationary discharge with shaped electrodes in argon, $p = 0.1$ torr; $B = 0.4$ kG.

gases (Ar, N_2 , SF_6 , He, and H_2) or their mixtures of various composition (argon percentage in Ar- N_2 and Ar- SF_6 composition ranged from 10 to 90%; He : $H_2 = 1 : 1$). We investigated the planar-magnetron and cusped-mirror configurations varying the magnetic field strength. We obtained current-voltage characteristics of the discharge, time-integrated photographs of the discharge glow, and probe characteristics of the discharge plasma. We detected the particle flux from the plasma and measured their intensities. As a result, we found out that a variety of regimes differing in discharge voltage, current range, and discharge space structure occurred.

Figure 3 shows typical voltage and current oscillograms of the quasi-stationary discharge. Part 1 in the voltage oscillogram represents the voltage of the stationary discharge (pre-ionization stage). Part 2a displays the square voltage pulse application to the gap. At this stage, the plasma density grows and reaches its quasi-stationary value (part 2b); the discharge current also grows, and then both the discharge current and voltage attain their quasi-stationary values (part 3). The time it takes for the plasma density to reach its quasi-stationary value corresponds to the ionization relaxation time. For example, for argon, discharge when pre-ionization plasma density is about $10^9 - 10^{11}$ cm^{-3} this time is about 50 μ s. Each point of the discharge characteristic represents a pair of voltage and current oscillograms. We detected inhomogeneity of the discharge plasma or cathode spots visually, using filters, or by photographing the discharge.

The current-voltage characteristic of the low-pressure quasi-stationary discharge in a magnetic field had four different parts corresponding to stable forms of the discharge. Figure 4 shows a typical CVC of the discharge in argon at 10^{-1} torr pressure and 0.4 kG magnetic field. One can differentiate two parts: part 1 corresponds to the magnetron discharge with current up to 0.2 A and voltage range from 260 to 280 V; part 4 corresponds to the high-current low-voltage arc discharge of current greater than 1 kA and 10 - 30 V voltage with a cathode spot. In addition, we found out experimentally that two other stable forms of quasi-stationary discharge could exist. Both the plasma and cathode layer had a diffuse character at cathode current density much higher than that of typical magnetron discharge. If the discharge current ranged from 0.2 to 15 A, a high-current magnetron discharge having initial discharge characteristics was observed (part 2 of the oscillogram).

In this case the discharge voltage was rather high, approximately 350 - 500 V. If the current was increased and ranged from 15 to 1000 A, a diffuse regime of high-current discharge was observed (part 3); its CVC was a straight line parallel to the current axis. The discharge voltage was about 90 V over the current range. The cathode current density was about 50 A/cm².

It should be noted that the boundaries of regimes could vary depending on the discharge conditions, e.g., on pressure, magnetic field strength, etc. Then, we studied regimes 2 and 3 separately to determine the boundary parameters of their occurrence, such as current, voltage, pressure, and magnetic field.

We studied the regimes both in the planar magnetron and shaped-electrode system geometries and found out that both regimes could occur regardless of the type or particular parameters of the discharge configuration.

Figure 5a exhibits representative CVC of the high-current magnetron discharge. They were measured in the discharge in Ar and N₂, as well as in or Ar-N₂ (10 - 90% of argon) or He : H₂ = 1 : 1 mixtures at 10⁻³ - 10 torr pressure range and 0.4 - 1.0 kG magnetic field. The cathodes we used were made of Cu, Ti, Al, Mo, or stainless steel. To reduce the effect of cathode surface quality on the discharge parameters, the electrodes were preconditioned by multiple discharges or cleaned by glow discharge in argon. The dependence $U_d(I_d)$ remained qualitatively the same for all values of were the pressure p , transverse magnetic field B_{\perp} , sort of the gas, cathode material, electrode configuration and discharge size. The discharge voltage increased monotonically with current up to a maximum $U_d^{\max} \approx 500 - 1100$ V depending on the magnetic field strength, sort of the gas, and cathode material. Then the discharge transferred to regime 3 or to the arc regime. If the voltage pulse duration τ was less than 20 ms, the current of transition amounted to 250 A, which corresponded to 25 A/cm² cathode current density j . A decrease in magnetic field strength resulted in an increase in the discharge voltage $U_d^{\max}(B_{\perp})$ up to some value U_d^{II} depending only on the cathode material and sort of the gas. A further decrease in B_{\perp} caused the discharge to transit to a high-voltage regime which was characterized by a steep CVC and low discharge current (about 1 A).

As the decreasing magnetic field approached the value of the discharge transit to the high-voltage regime, the discharge voltage increased smoothly, and the discharge current decreased.

We measured the CVC of the high-current magnetron discharge for two different discharge diameters. The CVC turned out to be independent of the diameter in the max B_r region. It should be noted that, being transferred to the high-current regime, the discharge expands over a considerably larger area of the cathode surface than it occupied in the stationary pre-ionization regime. In the case of the planar magnetron, the dis-

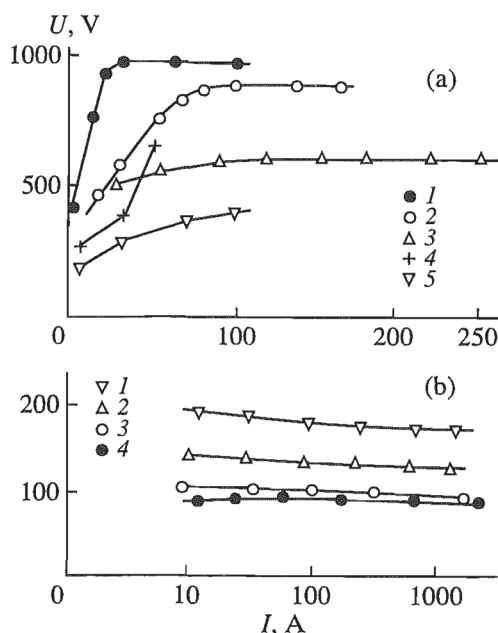


Fig. 5. (a) High-current magnetron discharge: (1) planar magnetron, Cu, $p = 5 \times 10^{-3}$ torr, Ar; (2) planar magnetron, Ti, $p = 5 \times 10^{-3}$ torr, Ar : N₂ = 4 : 1; (3) planar magnetron, Ti, $p = 10^{-2}$ torr, N₂; (4 and 5) shaped-electrode system, Cu, $p = 5 \times 10^{-2}$ torr, He : H₂ = 1 : 1, and Cu, $p = 10^{-1}$ torr, Ar. (b) High-current diffuse regime: (1 and 2) shaped-electrode system, Cu, $p = 1$ torr, He : H₂ = 1 : 1 and Cu, $p = 10^{-1}$ torr, He : H₂ = 1 : 1; (3) planar magnetron, Cu, $p = 10^{-1}$ torr, Ar; (4) planar magnetron, Cu, $p = 10^{-1}$ torr, Ar : SF₆ = 4 : 1.

charge occupied either the ring area beyond the circular region of max B_r or the disk area bounded by the circle of max B_r ; the area depended on the magnetic field configuration. Because the discharge current was the same in both cases, the current densities differed considerably, but the CVCs were similar. The current density values characteristic of these regimes for the argon discharges were $j = 4$ A/cm² ($U_d = 540$ V, $I_d = 225$ A) and $j = 25$ A/cm² ($U_d = 500$ V, $I_d = 218$ A).

The roughness of the cathode surface was not important for the occurrence of regime 2, though the probability of discharge transit to the arc discharge was greater for the cathodes with rougher surfaces.

A feature of the shaped-electrode discharges in the He-H₂ mixture was a second form of high-current magnetron regime at a 400 - 650 V discharge voltage that was independent of discharge current until transferring to regime 3.

Regime 2 was characterized by an intense cathode sputtering due to both high energy and density of ion flow. To study the sputtering, we used a probecollector placed 120 mm from the cathode. The pulsed deposition rate of cathode material (copper was used) turned out to be about 80 $\mu\text{m}/\text{min}$ in the argon discharge, $I_d = 65$ A, $U_d = 900$ V. The current pulse duration was 25 ms, and

the repetition frequency was 10 Hz, which corresponded to $\approx 20 \mu\text{m}/\text{min}$ averaged deposition rate. We used a scanning electron microscope REM-101 (Russian trade mark) to measure the thickness of deposited layers.

We measured the plasma density n_i in the region near the collector by applying to the collector a pulse of biased voltage with respect to the anode. The density turned out to be about $3 \times 10^{12} \text{ cm}^{-3}$ in the regime of $I_d = 60 \text{ A}$ and $U_d = 900 \text{ V}$.

Figure 5b presents typical CVCs of high-current diffuse discharge measured at various pressures, gases, cathode materials, magnetic fields, and pre-ionization parameters. Analyzing the CVCs, we found out that the discharge voltage weakly depended on the magnetic field geometry and its strength, and on the cathode material; the constant voltage turned out to range from 70 to 140 V as the current ranged from 5 to 1800 A. The voltage was slightly (within 50 V) changed from gas to gas. Transferring to regime 3, the discharge occupied a significantly larger cathode surface than in the stationary regime.

The parameters of the shaped-electrode discharge transit to regime 3, as well as the condition of its transit to arc regime 4, could be well determined for every given set of the discharge parameters. The point of the planar-magnetron discharge transit to the arc regime was determined by discharge voltage and structure changes; the structure changes were recorded by optical diagnostics. To study the structure of the discharge in regime 3, we photographed it using neutral light filters of various attenuation factors. The filters and exposure times were chosen so that the pre-ionization discharge glow was not recorded. One can see from the photographs presented in Fig. 6 that the discharge was spatially uniform even at about 1 kA discharge currents. If the current was raised above 1.8 kA or the pulse duration was increased to 2 - 10 ms, an instability development and discharge contraction was observed. The planar-magnetron discharge transfer to regime 3 resulted in a smearing of the annular structure of the pre-ionization discharge: the discharge plasma and current area were seen to expand and cover the whole cathode surface (Fig. 6). If the discharge current or pulse duration were increased, the instability development accompanied by the plasma column contraction and the occurrence of one of several cathode spots were also observed in the planar magnetron.

Chemical analysis of the collector surface layer was done; the cathode material was not detected there. Hence, there was no cathode sputtering in these regimes.

We elaborated on a pulsed probe technique specially designed to measure the plasma parameters in regime 3. The technique provided probe characteristics to be measured in $\approx 10 \mu\text{s}$ time intervals and allowed the probe current to amount to 50 A [10].

We measured the parameters of pulsed high-current quasi-stationary discharge in a cusp magnetic-field configuration with B ranging from zero to 1 kG in various gases. The pressure ranged from 10^{-1} to 1 torr; the discharge current ranged up to 1500 A. The pulse voltage applied to the probe was 100 - 500 μs delayed with respect to the discharge current pulse, i.e., T_e and n_i were measured after the establishment of the quasi-stationary regime of the high-current discharge.

The plasma parameters were determined from the probe measurements. Ion density measured at the system center in regime 3 in argon increased almost linearly with the discharge current at various pressures and magnetic field strengths. The density ranged from $(2 - 2.5) \times 10^{14} \text{ cm}^{-3}$ at 360 - 540 A current up to $(1 - 1.5) \times 10^{15} \text{ cm}^{-3}$ at 1100 - 1400 A current. The maximal plasma density of high-current diffuse discharge in argon was measured to be $n_i \approx 1.5 \times 10^{15} \text{ cm}^{-3}$, while the electron temperature T_e was 4 - 6 eV, the discharge current was 1100 A, magnetic field strength B was 0.8 kG, and the pressure p was about 0.2 torr. The ion saturation current of the probe j_{sat} was about 11 A/cm². Ion density increased with pressure; the density increase was accompanied by a decrease in the electron temperature.

The plasma density in He-H₂ discharge also increased with the discharge current. However, the maximum of ion density was $n_i = 2.4 \times 10^{14} \text{ cm}^{-3}$ at the conditions similar to those mentioned above: $p = 1.5$ torr, $B = 0.8 \text{ kG}$, $I_d \approx 1100 \text{ A}$.

4. DISCUSSION

We obtained a generalized CVC of the quasi-stationary low-pressure discharge in a magnetic field (Fig. 7) based on a variety of measured AV discharge characteristics under various conditions. Parts 1 and 4 correspond to stationary magnetron and arc discharges, respectively. They were inherent in the discharge throughout the pressure and magnetic field ranges. These two regimes were comprehensively described in [1, 11].

Part 2 pertains to the high-current magnetron discharge regime occurring in the 0.2 - 250 A current range. The voltage increased with current up to some critical value of current and then became constant. The discharge voltage was rather high - up to 1.2 kV. The discharge had a greater probability of being realized if the pressure ranged from 2×10^{-3} to 10^{-1} torr.

We suggested that this discharge was structurally very close to the high-current discharge described in [4]. The reasons are the following: both the pressure and magnetic field ranges were almost the same, the discharge did not exhibit contraction, and their CVCs were very similar. However, the discharge we dealt with had a higher discharge voltage (500 - 1200 V) than the 300 - 500 V discharge described in [4]. Hence, one could expect the cathode sputtering to have more importance.

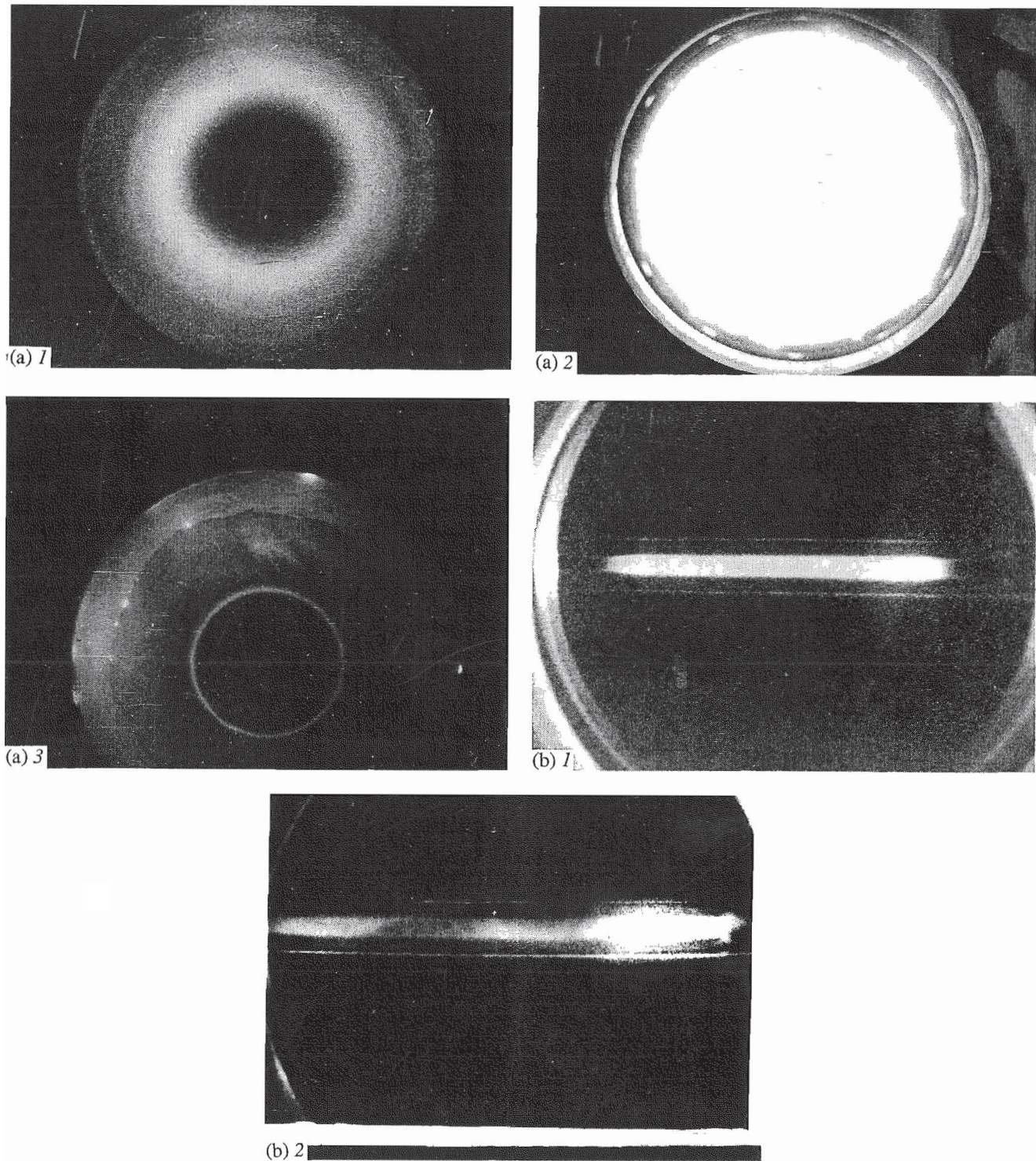


Fig. 6. High-current quasi-stationary discharge regimes. (a) planar magnetron: (1) high-current magnetron regime ($p = 5 \times 10^{-3}$ torr, Ar, $I_d = 70$ A, $U_d = 900$ V); (2) high-current diffuse regime ($p = 10^{-1}$ torr, Ar, $I_d = 700$ A, $U_d = 80$ V); (3) arc regime ($p = 10^{-1}$ torr, Ar, $I_d = 1000$ A, $U_d = 45$ V). (b) Shaped-electrode system: (1) high-current diffuse regime ($p = 10^{-1}$ torr, Ar, $I_d = 1000$ A, $U_d = 90$ V); (2) contracted arc regime ($p = 10^{-1}$ torr, Ar, $I_d = 1500$ A, $U_d = 50$ V).

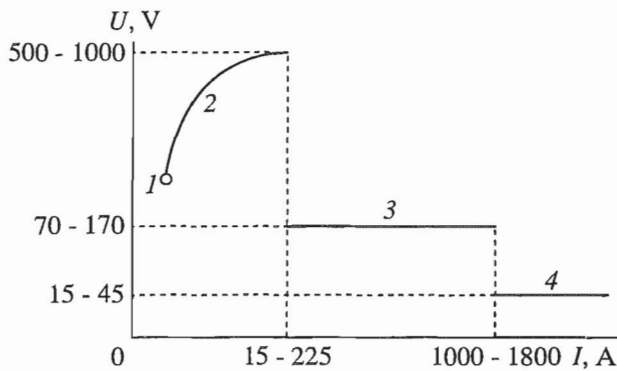


Fig. 7. Generalized ampere-voltic characteristic CVC of quasi-stationary discharge.

We estimated the steady-state average density of the cathode material atoms n_c in the discharge plasma; the estimates were based on measured current density and initial working gas density n_g . Using a one-dimensional continuity equation, it is possible to derive the following equation for n_c :

$$t \frac{\partial n_c}{\partial t} + n_c = S_{g-c} \beta_g n_g \frac{V_g^T}{\langle V_c \rangle} + \frac{1}{4} S_{c-c} \beta_c n_c \frac{V_c^T}{\langle V_c \rangle}, \quad (1)$$

where S_{g-c} and S_{c-c} are sputtering and self-sputtering factors of the cathode, respectively; V_g^T and V_c^T are thermal velocities of working gas atoms and cathode material atoms, respectively; $\langle V_c \rangle$ is the angle-averaged emitted atom velocity-component perpendicular to the cathode surface; β_g and β_c are ionization degrees of gas atoms and cathode material atoms, respectively.

The steady-state solution of (1) is as follows:

$$n_c = \frac{\frac{1}{4} S_{g-c} \beta_g n_g \frac{V_g^T}{\langle V_c \rangle}}{1 - \frac{1}{4} S_{c-c} \beta_c \frac{V_c^T}{\langle V_c \rangle}}.$$

As an example, we considered the copper-cathode argon discharge at 10^{-2} torr, $I_d = 65$ A, and $U_d = 900$ V

and estimated the copper fraction in its plasma. The fraction turned out to be about 30% and increased with ionization degree.

Table 1 presents the parameter ranges corresponding to regime 2. The presented parameters are limiting values that could be independently realized.

If the discharge current ranged from 10 to 1800 A, high-current diffuse regime 3 occurred. The voltage ranged from 70 to 140 V depending on the working gas sort. Regime 3 could be primarily realized in the 10^{-2} - 5 torr pressure range no matter what the discharge electrode configuration, sort of working gas, or cathode material. Moreover, pre-ionization was not necessary; however, in this case, the probability of discharge transferring to arc mode increased. The cathode current density of the high-current diffuse discharge amounted to 75 A/cm^2 .

Table 2 presents the parameter ranges corresponding to regime 3 for both electrode configurations; various cathode materials, and various pressures and sorts of gases.

It should be emphasized that the limiting values of regime 2 and regime 3 parameters were highly dependent on current pulse duration. The transit current values increased with a decrease in the pulse duration.

The process of the high-current magnetron discharge passing to a low-voltage regime seemed likely to resemble the anomalous glow discharge at moderate or high current densities [11]. In this case both the gas heating and electron density increase were important; these factors promoted both a partial equilibrium in the discharge plasma, and the transfer of the discharge to a regime of lower discharge voltage.

The simplified quasi-stationary equation for gas temperature of regime 2 has the form [9]:

$$(T_g - T_0) M_g C_p v_T = P_g, \quad (2)$$

where P_g is the power consumed to heat the gas; T_g is the established gas temperature; T_0 is the electrode temperature; M_g is the mass of the gas in the discharge volume; C_p is the heat capacity at constant pressure; $v_T =$

Table 1. Existence conditions and regimes of high-current magnetron discharge: (I) shaped-electrode system; (II) planar magnetron

Discharge device type	Cathode material	Gas	B , kG	Pressure, torr	Voltage, V	Current, A
I	Cu	Ar	0.4 - 1.0	10^{-2} - 10^{-1}	260 - 990	0.2 - 15
	Cu	He/H ₂ 50/50%	0.4 - 1.0	5×10^{-2} - 1	320 - 950	0.2 - 36
	Cu	He/H ₂ 50/50%	0.8 - 1.0	5×10^{-2} - 1	400 - 650	9 - 120
II	Cu	Ar	0.3 - 0.7	10^{-3} - 5×10^{-1}	540 - 990	0.2 - 72
	Ti	Ar	0.3 - 0.7	10^{-3} - 5×10^{-1}	540 - 1100	0.2 - 250
	Ti	N ₂	0.3 - 0.7	10^{-3} - 5×10^{-1}	540 - 720	0.2 - 180
	Ti	Ar/N ₂ 90 - 10% Ar	0.3 - 0.7	10^{-3} - 5×10^{-1}	540 - 900	0.2 - 140

Table 2. Existence conditions and regimes of high-current diffuse discharge: (I) shaped-electrode system; (II) planar magnetron

Discharge device type	Cathode material	Gas	B , kG	Pressure, torr	Voltage, V	Current, A
I	Cu	Ar	0.4 - 1.0	10^{-2} - 5	80 - 110	15 - 1500
	Cu	Ar/SF ₆ 80/20%	0.4 - 1.0	2×10^{-2} - 3	80 - 120	7 - 1200
	Cu	He/H ₂ 50/50%	0.8 - 1.0	5×10^{-2} - 3	70 - 120	7 - 1800
II	Cu	Ar	0.3 - 0.7	10^{-2} - 1	65 - 90	4 - 800
	Mo	Ar	0.3 - 0.7	5×10^{-2} - 1	65 - 90	4 - 1200
	Mo	Ar/SF ₆ 80/20%	0.3 - 0.7	10^{-2} - 1	90 - 135	18 - 1800
	Mo	SF ₆	0.3 - 0.7	10^{-2} - 5×10^{-1}	90 - 135	4 - 1600
	stainless steel	Ar/SF ₆ 80/20%	0.3 - 0.7	10^{-2} - 1	90 - 135	18 - 1200

χ/Λ_T^2 is the frequency characteristic of the heat evacuation; $\chi = \lambda/(Mn_g C_p)$ is the temperature conductivity; Λ_T is a characteristic heat evacuation length; λ is the gas thermal conductivity at the established temperature; M is atomic mass; and n_g is the gas density. The gas energy balance equation takes into account the discharge geometry, so the actual electrode profile was substituted for a plane one with area S and interelectrode distance L corresponding to the operating area in the regimes involved. As far as the plane discharge layer of $2L$ thickness is concerned, the value of Λ_T is about L/π . The power consumed for gas heating can be evaluated from the energy balance equation:

$$P_g = I_d U_d - \frac{I_d}{e\eta}, \quad (3)$$

where $I_d U_d$ is the total power released in the discharge volume; $I_d/e\eta$ is the power consumed for ionization; e is the electron charge; $1/\eta$ is the Stoletov constant corresponding to the value of E/n characteristic of the cathode layer.

The discharge conditions typical for the discharge transit from regime 2 to regime 3 are as follows: $I_d \approx 15$ A; $U_d \approx 300$ V; $p = 1$ torr; $B = 0$; argon was used as a working gas; $L \approx 1$ cm; and $S \approx 60$ cm². Under these conditions, the gas temperature could increase to $T_g \approx 1.1$ eV.

It follows from (2) that

$$T_g \approx \frac{P}{M_g C_p \nu_T} = \frac{1}{\pi^2} \frac{L}{S} \frac{I_d U_d - \frac{I_d}{e\eta}}{\lambda}, \quad (4)$$

i.e., that the gas temperature does not depend on gas density. The action of the magnetic field serves only to limit the electron thermal conductivity and to provide collisions sufficient for efficient energy transfer from electrons to heavy particles.

According to [11], one can evaluate the ionization degree from the Saha equation if ambipolar diffusion (A) is negligible, i.e., if plasma density is sufficiently high:

$n_e > n_e^{cr}$. The value of n_e^{cr} can be determined experimentally; it depends on the excitation energy of the first excited level.

If the cylindrical layer is considered, the averaged rate of charged particle rate due to diffusion can be described as follows [9]:

$$\left(\frac{\partial n}{\partial t}\right)_{dif} = D_A \Delta n = -\nu_D n \approx -\frac{D_A}{\Lambda^2} n, \quad (5)$$

where ν_D is the diffusion frequency; Λ is a characteristic length of diffusion depending on the discharge geometry. In the presence of a magnetic field, Λ is dictated by the highest of the frequencies determining the particle loss at the electrodes $\nu_{Dl} \approx \frac{(T_e + T_i)(\nu_{ea} + \nu_{ei})}{m\omega_e^2 + (\nu_{ea} + \nu_{ei})\mu_{ia}\nu_{ia}} \left(\frac{\pi}{L}\right)^2 n_e$ and at the lateral sur-

face of the discharge volume $\nu_{Ds} \approx \frac{(T_e + T_i)}{\mu_{ia}\nu_{ia}} \left(\frac{2.4}{R}\right)^2$

[12]. Here, R is the discharge radius; ω_e is the electron cyclotron frequency; ν_{ea} , ν_{ei} , and ν_{ia} are the frequencies of electron-atom, electron-ion, and ion-atom collisions, respectively; μ_{ia} is the reduced mass. One can compare the frequencies of diffusion, ionization, and recombination in argon discharge and, then, find out of establishing a detailed balance the possibility in the discharge plasma.

The estimates of the plasma density, in the case $T = T_g = T_i = 1.1$ eV, show that, according to [9], the following relation is valid:

$$\frac{\alpha^2}{1 - \alpha^2} = \frac{g_i}{g_g} \left(\frac{2\pi m}{h^2}\right)^{3/2} \frac{(kT)^{3/2}}{n_g + n_i} \exp\left\{-\frac{eU_i}{kT}\right\}, \quad (6)$$

where $g_i = 6$ (Ar) and $g_g = 1$ are the statistical weights of ions and atoms, respectively; U_i is the argon ionization potential. The ionization degree $\alpha = n_e/(n_g + n_i)$ ranges from $\alpha \approx 1$ ($p = 0.01$ torr) to $\alpha \approx 0.7$ ($p = 1$ torr),

i.e., the plasma density in the discharge passing to regime 3 exceeds $n_e \geq 5 \times 10^{13} \text{ cm}^{-3}$.

According to [9], the thermal ionization requires far less discharge voltage than electron impact ionization for current sustainment. This appears to cause the discharge to transfer to the low-voltage regime.

One can estimate both the gas temperature and associated ionization degree from (2) - (4) and energy balance change. The balance equation for the power consumed by neutral gas heating in regime 3 is as follows:

$$P_g = I_d U_d - \frac{I_d}{e} (\mathcal{E}_i + \frac{3}{2} k T_e + \frac{3}{2} k T_i), \quad (7)$$

where \mathcal{E}_i is the ionization energy, because, unlike the case of (2), the fraction of energy lost due to charged particle escape increases with discharge current. Similarly to the column of arc plasma at moderate pressure, the ion temperature T_i could be assumed to be equal to the atom temperature T_g [9]. Because ions and atoms have the same mass, the ion energy loss for atom heating is high (average energy fraction lost by an ion in an elastic collision δ_{ig} is about unity). In addition, because ion mass is large, ions are poorly heated by the electric field; they, as well as atoms, gain energy primarily due to elastic collisions with electrons. Neglecting the electrode temperature $T_0 \ll T_g$ in regime 3, one can write the following:

$$T_g = \frac{I_d U_d - \frac{I_d}{e} (\mathcal{E}_i + \frac{3}{2} k T_e)}{M_g C_p \nu_T + \frac{3}{2} k \frac{I_d}{e}}. \quad (8)$$

Let us take, for example, the following typical parameters of regime 3: $I_d = 540 \text{ A}$; $U_d = 90 \text{ V}$; $p = 0.1 \text{ torr}$; $B = 0.8 \text{ kG}$. Then we obtain the gas temperature $T_g = 3.2 \text{ eV}$. In the case $I_d = 1500 \text{ A}$, the value of T_g turns out to be about 5.4 eV . The plasma voltage drops relevant to these cases can be estimated from the probe measurements. For instance, $U_p \approx 40 - 36.5 \text{ V}$, which corresponds to the gas temperature T_g which is about $3.2 - 8.5 \text{ eV}$. Evidently, this is an overestimated value due to the contribution of radiation heat loss from the discharge. However, it testifies to the possibility of the ionization degree being about unity in regime 3.

One can see from the experimental data that the discharge transit to the low-voltage regime is possible if the plasma density reaches some critical value N_e corresponding to a rather small Debye radius. This allows one to suggest a collisionless cathode layer in regime 3. Because the negative potential of the cathode is far higher than the potential of the insulated probe under the considered conditions, one can suggest that it is the ion saturation current partially compensated by electron emission that arrives at the cathode from the

plasma. Then, the positive space charge layer thickness at the cathode surface is determined as follows [9]:

$$l_c = \left(\frac{8}{9}\right)^{1/2} \left(\frac{M}{m}\right)^{1/4} \left(\frac{e U_c}{k T_e}\right)^{3/4} \left(\frac{k T_e}{4 \pi e^2 n_e}\right)^{1/2}. \quad (9)$$

We compared the value of l_c , which corresponds to the electron density of the discharge transfer to regime 3, with electron free path lengths λ_{ea} and λ_{ei} (high pressures) and with the trajectory height over the cathode surfaces $h_e = \frac{2 m c^2 \langle E_c \rangle}{e B_r^2}$ of electrons moving in crossed fields (low pressures) [13]. We determined that the above suggestion is valid throughout the ranges of discharge transit current, pressure, and magnetic field. Moreover, the increase in n_e with current appeared to strengthen the inequalities $l_c \leq \lambda_{ea}, \lambda_{ei}, h_e$.

The Poisson equation describing the collisionless discharge layer in regime 3 is similar to that describing the layer of the cold-cathode arc [9]:

$$\begin{aligned} -\frac{d^2 U}{dx^2} &= 4 \pi e (n_i - n_e), \quad j_e = S j = e n_e V_e, \\ j_i &= (1 - S) j = e n_i V_i, \quad V_e = \left(\frac{2 e U}{m}\right)^{1/2}, \\ V_i &= \left(\frac{2 e (U_c - U)}{M}\right)^{1/2}, \quad S = \frac{\gamma}{1 + \gamma} = \frac{j_e}{j_e + j_i}, \end{aligned} \quad (10)$$

where $\gamma = \gamma_{ie} + \gamma_{hv}$ is the secondary electron emission coefficient determined by both ion-electron emission and photoemission.

Assuming the electric field at the plasma boundary E_p to equal zero, one obtains the electric field strength at the cathode surface $U = U_c$

$$E_c = \left\{ \frac{16 \pi}{(2e)^{1/2}} [(1 - S) M^{1/2} - S m^{1/2}] \right\}^{1/2} \times U_c^{1/4} j^{1/2} \quad (11)$$

and, accordingly, the cathode voltage drop

$$U_c = \left\{ \frac{12 \pi}{(2e)^{1/2}} [(1 - S) M^{1/2} - S m^{1/2}] \right\}^{2/3} \times j^{2/3} l_c^{4/3}. \quad (12)$$

The plasma density determined from probe measurements turned out to depend almost linearly on the discharge current. In addition, $l_c \sim 1/n_e^{1/2}$, i.e. $U_c \sim j^{2/3} \{1/j^{1/2}\}^{4/3}$, does not depend on j ; this agrees with the results of our experiments.

It follows from the above consideration that the high-current quasi-stationary discharge with plasma density n_e higher than $10^{13} - 5 \times 10^{13} \text{ cm}^{-3}$ is characterized by the existence of a collisionless cathode layer. Its voltage depends only weakly on the current. There

is also an active plasma zone where the thermal ionization mechanism does prevail.

In low-pressure range $p < 0.01$ torr and moderate magnetic field $B < 1$ kG, the necessary plasma density does not appear to be generated in the discharge; therefore, the high-current magnetron discharge (regime 2) is realized only if its current is higher than the transit currents characteristic of regime 3 and then transfers immediately to the arc regime.

The anomalous glow-discharge cathode layer transferring to the regime of current densities intermediate between normal current densities and arc cathode spot ones was studied in [14]. A transition regime of the glow discharge was found out to exist in nitrogen, air, and helium at 20 - 760 torr. The cathode material was not detected in the discharge plasma; its characteristics such as discharge voltage and cathode current density turn out to be quite close to those of the high-current diffuse regime of the quasi-stationary discharge in crossed electric and magnetic fields, though the total discharge currents of these discharges – 1.5 A in glow discharge and 1800 A in the discharge we dealt with – differ significantly. Hence, one can expect that the cathode layer structure of the discharge in regime 3 is similar to that of the pre-arc cathode spot [14].

In conclusion, we note that the high-current diffuse regimes are efficient enough for technological applications. The implementation of the high-current magnetron discharge (regime 2) in sputtering or layer-deposition technologies provides an enhancement in the flux of deposited materials and plasma density (exceeding $2 \times 10^{13} \text{ cm}^{-3}$). Moreover, it can enhance the chemical purity and homogeneity of deposited layers by adjusting the time of treated material exposure to sputtering material flux, e.g., by choosing the exposure time that is less than either the time characteristic for heat transfer in a treated material or the characteristic time of chemical reactions on the treated surface. Furthermore, this makes it possible to dictate the thermal regime for treated material surfaces including non-heat-resistant ones.

The high-current diffuse discharge (regime 3) is useful for producing large-volume uniform dense plasmas $n_i \approx 1.5 \times 10^{15} \text{ cm}^{-3}$ with ion-electron temperature difference about 3 - 20 eV and for generating an intense (10 to 12 A/cm²) ion flux of up to 100 eV ion energy. Hence, it can enhance the efficiency of ionic etching in

microelectronics and provide a means for controlled pulsed etching of layers.

The authors are grateful to Yu.S. Akishev for fruitful discussions.

REFERENCES

1. Maniv, S. and Westwood, W.D., *J. Vacuum Sci. and Techn.*, 1980, vol. 17, p. 743.
2. Danilin, B.S., *Primenenie Nizkotemperaturnoi Plazmy dlya Naneseniya Tonkikh Plenok* (Low-Temperature Plasma Applications for Thin Layer Depositions), Moscow, 1989.
3. Oks, E.M. and Chagin, A.A., *Zh. Tekh. Fiz.*, 1991, vol. 61, p. 204.
4. Tyuryukanov, P.M., Fetisov, I.K., and Nikol'skii, A.D., *Zh. Tekh. Fiz.*, 1981, vol. 51, p. 2028.
5. Mozgrin, D.V., Fetisov, I.K., and Khodachenko, G.V., Abstracts of Papers, *I Vsesoyuznoe Soveshchanie po Plazmennoi Emissionnoi Elektronike* (I All-Union Seminar for Plasma Emission Electronics), Ulan-Ude, 1991, vol. 1, p. 32.
6. Mozgrin, D.V., Fetisov, I.K., and Khodachenko, G.V., Abstracts of Papers, *VI Konferentsiya po Fizike Gasovogo Razryada* (VI Conf. Gas Discharge Physics), Kazan, 1992, part 2, p. 192.
7. Fetisov, I.K., Khodachenko, G.V., and Mozgrin, D.V., Abstracts of Papers, *ICPIG-XX*, Pisa, 1991, vol. 2, p. 476.
8. Kudryavtsev, A.A. and Skrebov, V.N., *Zh. Tekh. Fiz.*, 1983, vol. 53, p. 53.
9. Raizer, Yu.P., *Fizika Gasovogo Razryada* (Physics of Gas Discharge), Moscow: Nauka, 1987.
10. Mozgrin, D.V., Fetisov, I.K., and Khodachenko, G.V., Abstracts of Papers, *VIII Vsesoyuznaya Konferentsiya po Fizike Nizkotemperaturnoi Plazmy* (VIII All-Union Conf. Low-Temperature Plasma Physics), Minsk, 1991.
11. Granovskii, V.L., *Elektricheskii Tok v Gazakh* (Electric Current in Gases), Moscow: Nauka, 1971.
12. Rozhanskii, V.A. and Tsendin, L.D., *Stolknovitel'nyi Perenos v Chastichno Ionizovannoi Plazme* (Collisional Transfer Processes in Partially Ionized Plasmas), Moscow: Energoatomizdat, 1988.
13. Korolev, L.V., Pavlyuchenko, D.I., Fetisov, I.K., and Khodachenko, G.V., *Fizika Gazorazryadnoi Plazmy* (Physics of Gas Discharge Plasmas), Tel'kovskii, V.G., Ed., Moscow: Energoatomizdat, 1984, p. 12.
14. Akishev, Yu.S., Napartovich, A.P., Ponomarenko, V.V., and Trushkin, Yu.S., *Zh. Tekh. Fiz.*, 1985, vol. 55, p. 655.